Invited Paper

An Accumulative X-ray Streak Camera with 280 fs Resolution

Mahendra Man Shakya and Zenghu Chang
J.R. Macdonald Laboratory, Department of Physics, Kansas State University, Manhattan, KS 66506

ABSTRACT

We demonstrated a significant improvement in the resolution of the x-ray streak camera by reducing the electron beam size in the deflection plates. This was accomplished by adding a slit in front of the focusing lens and the deflection plates. The temporal resolution reached 280 fs when the slit width was 5 μm. The camera was operated in an accumulative mode and tested by using a 25 fs laser with 2 kHz repetition rate and 1-2% RMS pulse energy stability. We conclude that deflection aberrations, which limit the resolution of the camera, can be appreciably reduced by eliminating the wide-angle electrons.

Keywords: streak camera, accumulation mode, deflection aberrations, timing jitter, photoconductive switch, ultrafast detector.

1. INTRODUCTION

The combination of the third generation x-ray sources and the picosecond x-ray streak cameras provide a powerful approach to study ultrafast dynamics in solids and in plasma, e. g. by heating of an InSb crystal with ultrafast laser pulses, Falcone and co-workers have observed the temporal oscillations in x-ray intensity caused by coherent lattice oscillation [1-3]. Ultrashort plasma x-ray sources produced from lasers can be used to probe in the pump-probe experiments to study similar phenomena [4, 5], however, it is time consuming to take data with a high-temporal resolution and a large time window. The x-ray streak camera covers a large time window. Had there been no such streak camera developed, coherent acoustic oscillations in the work of Berkeley [2] may not have been discovered.

Since the x-ray photon number in a single pulse from the third generation x-ray sources is low, the x-ray streak camera must be operated in an accumulation mode. In such mode, the temporal resolution is limited by the timing jitter between the laser that starts the ultrafast events and the streak camera that measures the events [1]. Liu *et al* [6] demonstrated that a camera with <100fs jitter by using a fast photoconductive switch. In this paper we report the improvement of the camera resolution by confining the electron beam size with a variable slit in the streak tube.

2. THE CAMERA DESIGN

The streak camera design is shown schematically in Fig. 1. There is a 25 μm slit on the anode that defines the field of view of the camera. A second slit in front of the electrostatic quadruple lens is for reducing the electron beam size in the lens and in the deflection plates. The lens images the anode slit in the sweeping direction only. When a streak camera operates in the accumulative mode, the main factors affecting the temporal resolution are the transit time dispersion, the scanning speed, the timing jitter, and the deflection aberrations. We discuss the first three items in this section and the deflection aberrations in the next section.

2.1 The transit time dispersion

For the x-ray streak camera, the dispersion is caused by the initial energy spread when the photoelectrons are released from the photocathode. It can be estimated by the equation

$$\Delta t_{pa} = \frac{2.63\sqrt{\delta\varepsilon}}{E} \qquad (1)$$

Fourth Generation X-Ray Sources and Optics II, edited by Sandra G. Biedron,
Wolfgang Eberhardt, Tetsuya Ishikawa, Roman O. Tatchyn, Proc. of SPIE Vol. 5534
(SPIE, Bellingham, WA, 2004) · 0277-786X/04/$15 · doi: 10.1117/12.560526

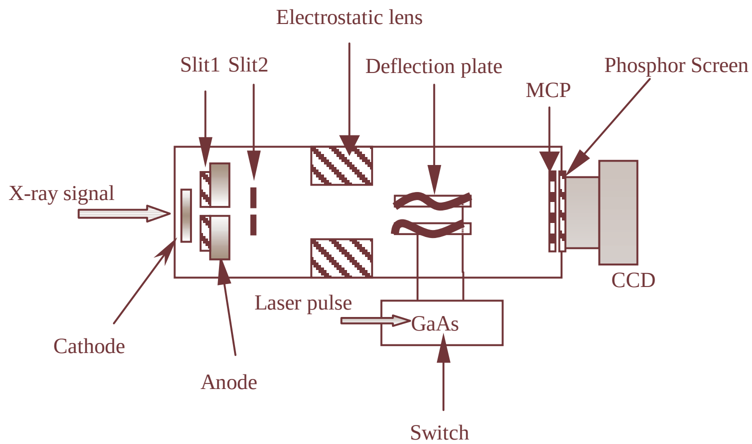

Fig. 1. Schematic of the x-ray streak camera with the variable slit.

where Δt_{pa} is in ps, $\delta\varepsilon$ is the FWHM of the energy distribution of the electrons in eV and the value is 0.5 eV for gold and E is an electric field at the cathode to anode region in kV/mm. To achieve 100 fs, the electric field must reach 18.6 kV/mm. The difficulty to reach such a high field is the arcing between the cathode to the anode. One solution to avoid arcing is to reduce the amount of residual gas in the streak tube. With our camera design, the electric field between the cathode and anode can be as high as 13.75 V/mm by reducing pressure to $2\text{x}10^{-9}$ torr, which yields $\Delta t_{pa} = 136$ fs.

2.2 The scanning speed

The effects of scanning speed, V, on the camera resolution can be express as

$$\Delta t_s = \Delta X / V \quad (2)$$

where ΔX is the static image width of the anode slit. By using a GaAs photoconductive switch and a meander type deflection plate, the scanning speed of the camera reached 0.84 μm/fs, i.e. 2.8 times of speed of light. Without the second slit, the image width $\Delta X = 166$ μm, as shown in Fig. 2. The width is much larger than the ideal value, 52.1μm, that is the product of anode slit width and the magnification of the streak tube. The broadening of the image width, was caused by the aberrations of the quadruple lens. The aberrations were reduced by reducing the electron beam size in the lens. The narrowing of the image width by the second slit was significant, as shown in Fig. 3. The narrowest image is 77 μm, obtained when the width of the 2nd slit was 5 μm, which is close to the ideal value.

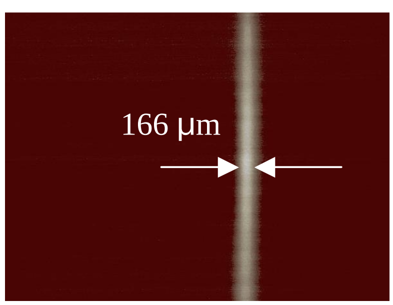

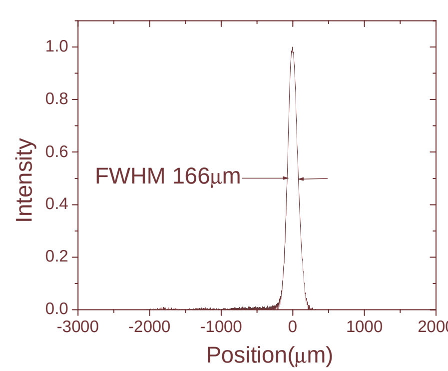

Fig. 2. The static image without the 2nd slit and its lineout of the static image

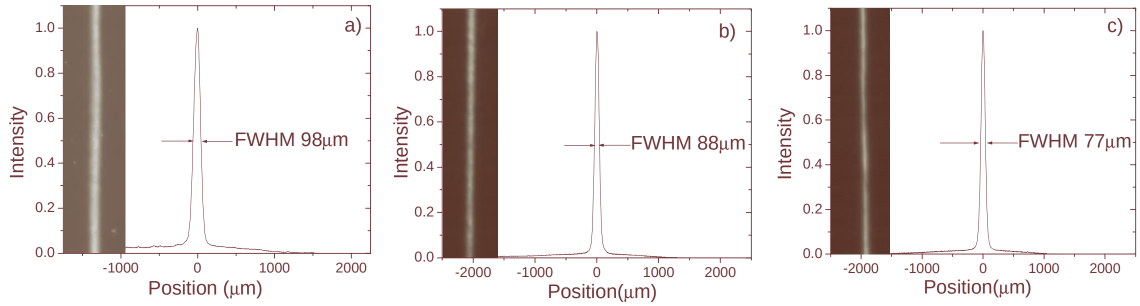

Fig. 3. The static images and their lineout when the 2nd slit width is: a) 50 mm, b) 25 mm, and c) 5 mm.

For the image width of 77 μm and the scanning speed of 0.84 μm/fs, the estimated resolution from equation (2) is 92 fs.

2.3 The timing jitter

A photoconductive switch is used to generate the ramp pulse for driving the deflection plates. The configuration of the camera is shown in Fig. 4, which is almost the same as in [7], except that the 2 GHz connection cables were replaced by the ones with a 18 GHz bandwidth to reduce the rise time from 90 ps to 60 ps. DP 1 and DP 2 are the deflection plates. $+V_0$ and $-V_0$ are the DC voltages applied to the switch. The photoconductive switch used in this experiment is made of semiconductor GaAs that has a resistivity of 10^{-7} Ω-cm. The active zone of this switch has the area of 0.5 cm^2. Contact resistance was reduced sufficiently by depositing electrodes on the switch with the 2 mm gap between them. The switch was mounted on a circuit board with 50 Ω transmission line, in an attempt to make response time as fast as possible and to eliminate the pulse reflection. The capacitance of the DC block is 1000 pf. As laser energy incident on the switch, it turns on and produces symmetric output to the deflection plates.

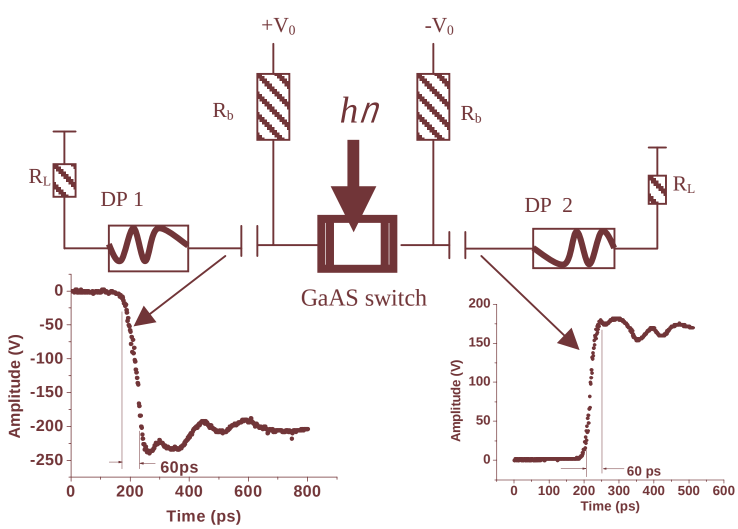

Fig. 4. Configuration of the photoconductive switch.

The timing jitter in the accumulative mode is caused by laser energy fluctuation. The output amplitude of the photoconductive switch saturates at high laser energy, as shown in Fig. 5. By operating the camera at the saturation regime, the fluctuation in the output voltage was less sensitive to the laser energy fluctuation. Thus the jitter can be reduced by setting the laser energy at the saturation range. For the test of the camera, the laser energy was set at 60 μJ. It was expected that jitter be less than 100 fs [6].

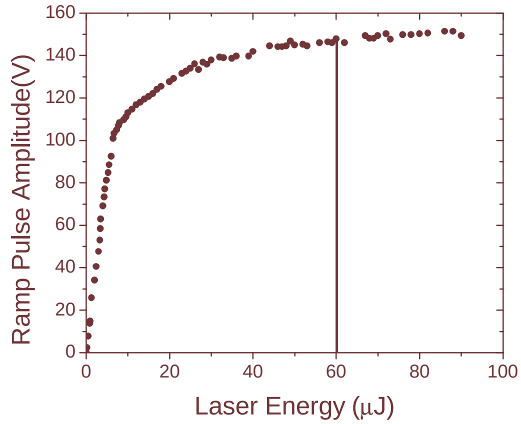

Fig. 5. The dependence of the pulse amplitude from the GaAs switch on the trigger laser energy

3. MEASUREMENT OF THE TEMPORAL RESOLUTION

The streak camera was tested at the Kansas Light Source facility. The system for charactering the camera is shown in Fig. 6. The Ti:Sapphire laser generates 25 fs pulses with 2 mJ energy at 2 kHz repetition rate. 85% of the total output was sent to a Mach-Zehnder interferometer. One beam from the interferometer was incident on the GaAs switch, which was mounted on a rail. In the mean time the other beam from the interferometer was used to produce photoelectrons. There were two pulses in each beam.

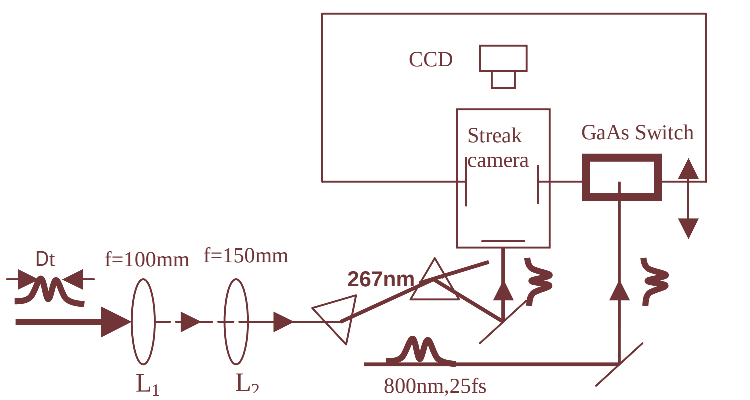

Fig.6 The layout of the setup for charactering the streak camera

The two pulses from one of the Mach-Zehnder interferometer output beam was focused by a lens with a focal length of 100 cm to produce third harmonic pulses in air. Another 125 cm focal length lens was used to image the UV source on the cathode. The 800nm/267nm beam was incident on a pair of prisms to separate UV from the infrared. Finally, the photoelectrons were generated by UV beam at the photocathode.

The dependence of the time resolution of the camera on the width of the 2^{nd} slit was studied. The results obtained when there was no 2^{nd} slit and the 2^{nd} slit width set at 50 µm, 25 µm and 5 µm are shown in Fig. 7(a), (b), (c) and (d) respectively. The results are summarized in Fig. 8. It clearly shows that resolution can be improved by reducing the width of the 2^{nd} slit. The best temporal resolution was obtained with the 5 μm slit. It was 280 fs by the conventional FWHM definition and 330 fs by the Rayleigh criterion (Fig. 7d). This result was obtained when the sweep speed was 2.8 times the velocity of the light and the laser stability of 1-2% RMS.

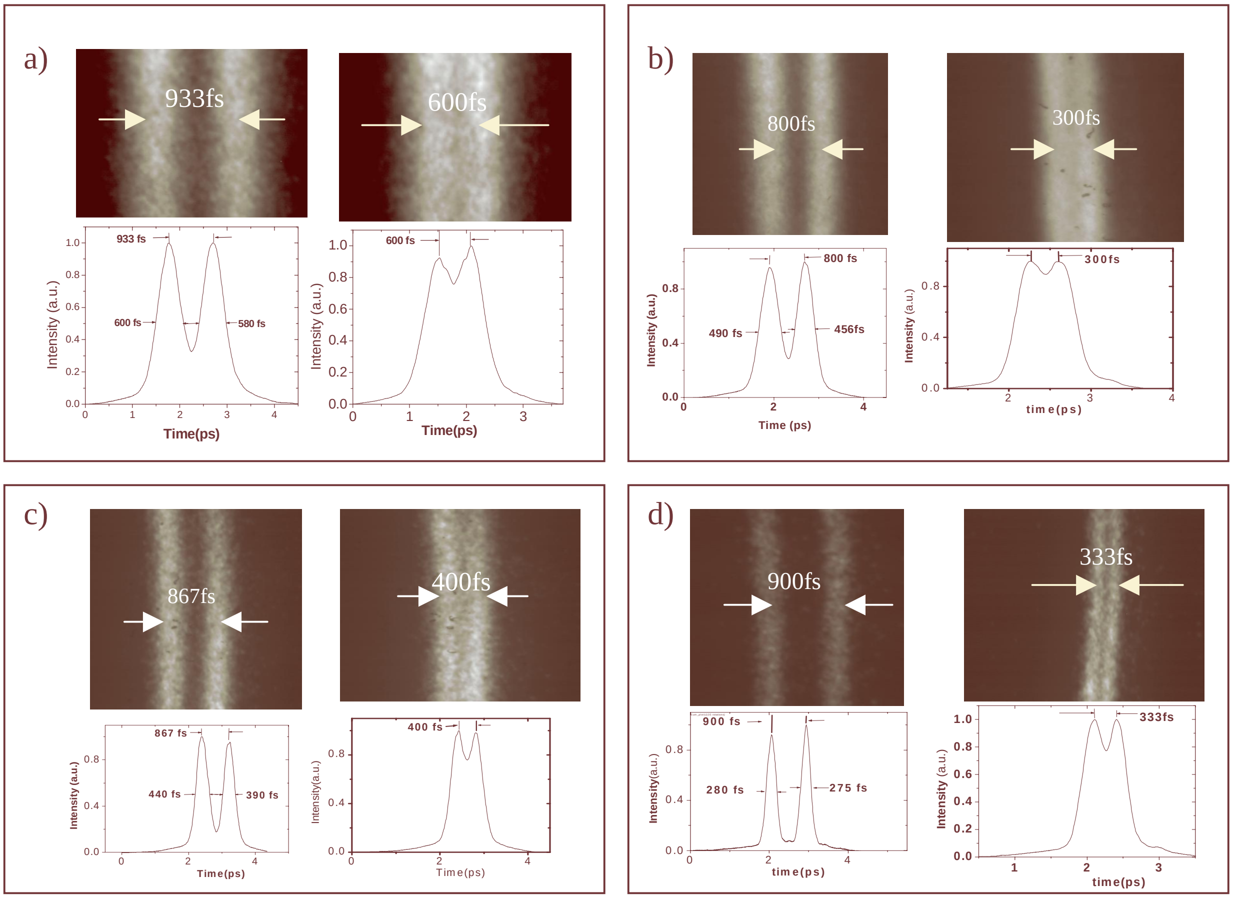

Fig. 7. Dynamic images when the 2^{nd} Slit was set a) open b) 50 μm c) 25 μm d) 5 μm

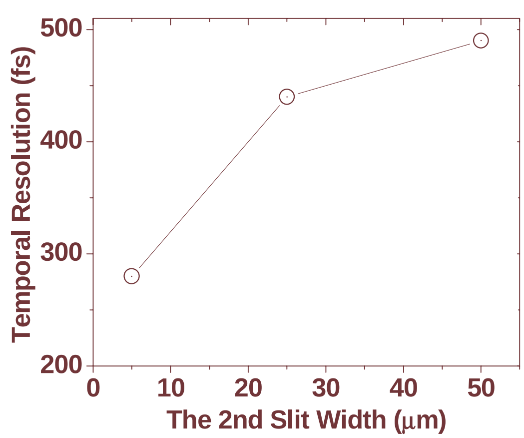

Fig. 8. The dependence of the camera resolution on the 2nd slit width.

The results suggest that the temporal resolution can be improved by reducing the size of the electron beam in the defection plates. The effect of the beam size, *d*, on the temporal resolution can be estimated by,

$$\Delta t_d = d\alpha / v_a \tag{3}$$

where α is the maximum deflection angle in radian and v_a is the average electron axial velocity. In our camera $\alpha = 0.015$ rad, $v_a = 1.6\times10^{-3}$ μm/fs. With the 5 μm width for the 2nd slit, the estimated dispersion caused by the deflection is on the order of 50 fs, which is much better than the measured value. The calculated resolution is 500 fs for a 50 μm slit, which is close to the measured value. The comparison between the measurement and estimation suggests that the contribution is a major limiting factor when the 2nd slit is wide. In the case of the 5 μm slit, other factors discussed in the previous section can not be neglected.

The price paid for improving the resolution was the reduction of the detected signal. This dependence of the signal on the slit width is shown in Fig. 9. For the camera that operates in an accumulative mode, the loss in the signal intensity can be recovered by increasing laser shots.

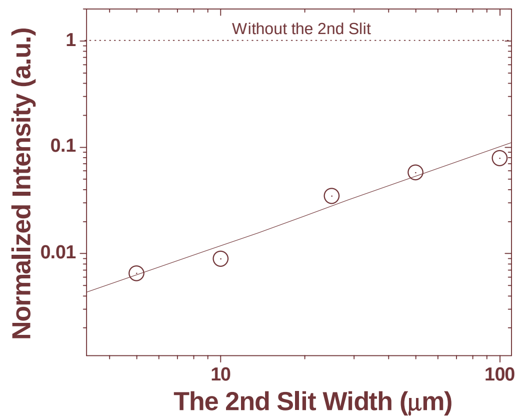

Fig. 9. The dependence of detected signal on the width of the 2nd slit

4. CONCLUSION

It was demonstrated the temporal resolution of a streak camera was significantly improved by reducing the electron beam size in the focusing lens and in the deflection plates. To the best of our knowledge, the 280 fs FWHM resolution is the best resolution ever achieved with a camera operating at the accumulation mode. X-ray cameras with such a high resolution will not only push the research at the third generation facility to a femtosecond level, but will also impact the development and applications of the fourth generation x-ray sources.

5. ACKNOWLEDGEMENT

This work is supported by the Division of Chemical Sciences, Office of Basic Energy Sciences, US Department of Energy. We would like to thank J. Liu for his invaluable help. The supports from B. Shan, C. Wang and J. Xia at the Kansas Light Source facility are greatly appreciated.

6. REFERENCES

1. J. Larsson, Z. Chang, E. Judd, P. J. Schuck, R. W. Falcone, P. A. Heimann, H. A. Padmore, H. C. Kapteyn, P. H. Bucksbaum, M. M. Murnane, R. W. Lee, A. Machacek, J. S. Wark, X. Liu and B. Shan, Optics Letters **22**, 1012 (1997).
2. A. M. Lindenberg, I. Kang, S. L. Johnson, T. Missalla, P. A. Heimann, Z. Chang, J. Larsson, P.H. Bucksbaum, H. C. Kapteyn, H. A. Padmore, R. W.Lee, J. S. Wark and R.W. Falcone, Phys. Rev. Lett. **84**, 111 (2000).
3. Z. Chang, A. Rundquist, J. Zhou, M. M .Murnane, H. C.Kapteyn, X. Liu, B. Shan, J. Liu, L. Niu, M. Gong and X. Zhang, Appl. Phys. Lett. **69**, 1(1996).
4. C.W. Siders, A. Cavalleri, K. Sokolowski-Tinten, C. Toth, T. Guo, M. Kammler, M.H. v. Hoegen, K.R. Wilson, D. v. d. Linde, and C.P.J. Barty, Science **286**, 1340 (1999).
5. C. Rose-Petruck, C. R. Jimenez, T. Guo, A .Cavalleri, C.W. Siders, F. Raski, J.A. Squier, B.C. Walker, K. Wilson, and C.P.J. Barty, Nature (London) **398**, 310(1999).
6. Jinyuan Liu, Jin Wang, Bing Shan, Chun Wang, and Zenghu Chang, Appl. Phys. Lett. **82**, 3553 (2003).
7. J. Liu, A. G. MacPhee, J.Wang, B. Shan, , C. Wang and Z. Chang , Proceedings of SPIE **4796**, 184 (2003).